

## Fractalkine Targeting with a Receptor-Mimicking Peptide-Amphiphile

Efrosini Kokkoli,\*<sup>†</sup> Rachel W. Kasinskas,<sup>‡</sup> Anastasia Mardilovich,<sup>†</sup> and Ashish Garg<sup>†</sup>

Department of Chemical Engineering and Materials Science, University of Minnesota, Minneapolis, Minnesota 55455, and Department of Chemical Engineering, University of Massachusetts, Amherst, Massachusetts 01003

Received October 13, 2004; Revised Manuscript Received January 16, 2005

In this study we have designed the NTFR peptide-amphiphile that mimics a fragment of the N-terminus of the fractalkine receptor (CX<sub>3</sub>CR1) and specifically targets fractalkine, a novel adhesion molecule expressed on the surface of inflamed endothelial cells. Bioartificial membranes were constructed from mixtures of NTFR peptide-amphiphiles and DPPC (1,2-dipalmitoyl-*sn*-glycero-3-phosphocholine) phospholipids, and the affinity and specificity of fractalkine for the synthetic NTFR was investigated with an atomic force microscope (AFM). Fractalkine was immobilized onto the AFM tips, and forces were collected between fractalkine and the bioartificial membranes. The adhesive interactions were studied at the collective level, when each adhesion event corresponded to the rupture of multiple biomolecular bonds. Retraction force profiles for the fractalkine–NTFR system exhibited single or multiple peaks and a small percentage of the force curves demonstrated stretching of the fractalkine–NTFR complex. Strong adhesion was measured when both DPPC and NTFR were present, compared to pure NTFR surfaces. This may be due to the fact that the DPPC molecule is shorter, and thus it can provide more space for the peptide headgroup to bend and expose its sequence at the interface. Specificity was demonstrated by comparing the NTFR–fractalkine adhesion to the forces between the  $\alpha_5\beta_1$  integrin (an adhesion receptor expressed on the surface of endothelial cells) and other surfaces such as GRGDSP (the specific ligand for  $\alpha_5\beta_1$ ), GRGESP (an inactive sequence), and NTFR.

### Introduction

Over the past decade we have witnessed an explosion in research aimed at creating new and improved drug delivery systems driven by a strong need in clinical practice. Advances in materials science and biotechnology are permitting the development of new physical and chemical methods of drug delivery. Currently, the main problems associated with systemic drug administration are the necessity of a large drug dose to achieve high local concentration, adverse side effects due to high drug doses, even biodistribution throughout the body, and lack of specific affinity for the pathological site.<sup>1</sup> Drug targeting can bring a solution to all these problems.

For two decades the liposome has been portrayed as “the magic bullet”. A targeting ligand would be immobilized at the liposome surface, so that it would specifically bind only to the target tissue.<sup>2</sup> Liposomes have been investigated extensively and long-circulating liposomes (stealth liposomes) have recently gained increased attention as systemic drug delivery vehicles as a result of regulatory approval of several liposome-based pharmaceutical products for parenteral administration.<sup>3,4</sup> For improvement in site-specific delivery

of clinical active stealth liposomes, delivery systems need to include site-directed surface ligands.

Our approach focuses on designing and engineering peptide-amphiphiles that specifically target fractalkine, a novel adhesion molecule on the surface of endothelial cells. Fractalkine (neurotactin, CX<sub>3</sub>CL1) is a recently discovered chemokine present on activated endothelium, epithelium, dendritic cells, and neurons.<sup>5–9</sup> It contains a unique CX<sub>3</sub>C motif, with three amino acids between the first two cysteines. In contrast to chemokines that are only present in soluble form, fractalkine can exist in two forms: either as a membrane-bound molecule, where it is anchored to vascular wall cells by an extended mucin stalk (Figure 1A) linked to a transmembrane domain (not shown in Figure 1A), or as a freely diffusible form (soluble fractalkine). Due to its unique molecular structure, fractalkine exhibits all the chemokine activities that the other chemokine molecules have and in addition it acts as an adhesion molecule for leukocytes. Previous studies have shown that the binding of fractalkine with its receptor (CX<sub>3</sub>CR1) is of high affinity with a dissociation constant ( $K_d$ ) of 30–740 pM.<sup>10–14</sup> The wide range of  $K_d$  values in the literature is probably due to the use of different experimental systems and assay methods.<sup>13</sup>

Fractalkine and its receptor (CX<sub>3</sub>CR1) may suggest a new mechanism of leukocyte adhesion and extravasation at the leukocyte–endothelial cell interface and define new targets for development of antiinflammatory agents. More impor-

\* To whom correspondence should be addressed: e-mail kokkoli@cems.umn.edu; fax (612) 626-1185.

<sup>†</sup> University of Minnesota.

<sup>‡</sup> University of Massachusetts.

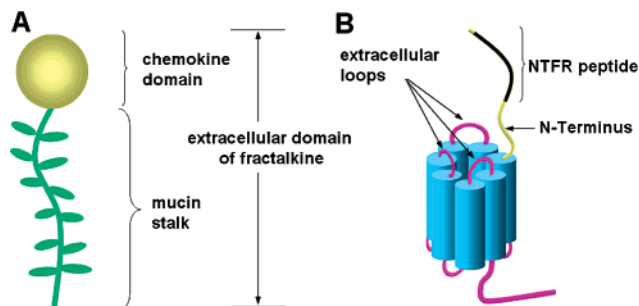


**Figure 1.** (A) Schematic representation of the extracellular domain of fractalkine (not drawn to scale). The chemokine domain is sitting on top of a mucin stalk. (B) Schematic representation of the CX<sub>3</sub>CR1 fractalkine receptor (not drawn to scale). The location of the NTFR peptide on the N-terminus is shown.

tantly, within the vascular system fractalkine is expressed only at sites of infection or inflammation; thus it can serve as a specific target moiety for drug delivery targeting. Our approach will utilize fractalkine as the target site and a peptide that mimics a fragment of the CX<sub>3</sub>CR1 fractalkine receptor as the magic bullet.

The N-terminal regions of several chemokine receptors are involved in chemokine binding and specificity.<sup>15–21</sup> For example, chimeric receptors in which the N-terminus of one chemokine receptor is replaced by that of another have been shown to exhibit specificity dictated by the N-terminal fragment.<sup>16,18,19</sup> In addition, the N-terminal segments of chemokine receptors alone may impart significant affinity for the ligand.<sup>17</sup> These observations have prompted the use of N-terminal receptor-derived peptides to model the interaction between chemokines and their receptors. Testing of the N-terminal peptides of CCR3, CXCR1, and CX<sub>3</sub>CR1 by NMR titration have shown binding to eotaxin or eotaxin-2, interleukin 8 (IL-8), and the chemokine domain of fractalkine, respectively.<sup>22–26</sup> For the study involving the CX<sub>3</sub>CR1 receptor, a peptide was used that corresponded to residues 2–19 of the N-terminus of CX<sub>3</sub>CR1 (the NTFR peptide corresponds to residues 3–20 of the N-terminus of CX<sub>3</sub>CR1), and its binding with only the chemokine domain of the fractalkine molecule was shown to be relatively weak (micromolar to millimolar)<sup>24</sup> compared to the affinity of the whole receptor CX<sub>3</sub>CR1 for the whole fractalkine molecule, which is in the range of 30–740 pM.<sup>10–14</sup> A recent study demonstrating that CX<sub>3</sub>CR1 tyrosine sulfation increases fractalkine binding showed that the affinity of the whole fractalkine molecule for the N-terminal peptide corresponding to residues 1–20 was high, with  $K_d = 6.6$  nM, and was increased approximately 10-fold when the peptide was sulfated with a SO<sub>3</sub>H<sub>2</sub> group added to the tyrosine residue (Tyr-14) with  $K_d = 0.79$  nM.<sup>14</sup>

For the development of a fractalkine-targeted drug delivery system we will focus on the N-terminus of CX<sub>3</sub>CR1, the fractalkine receptor. The design is based on the hypothesis that a peptide-amphiphile that mimics a fragment of the N-terminus of the fractalkine receptor (NTFR peptide-amphiphile) will recognize and specifically bind to fractalkine, thus localizing only at sites of inflammation or infection. Figure 1B gives a schematic representation of the CX<sub>3</sub>CR1 receptor and the location of the NTFR peptide.

In this study bioartificial membranes that mimic the surface of a liposome are constructed from mixtures of NTFR peptide-amphiphiles and DPPC phospholipids. The peptide-amphiphile structure includes a dialkyl ester tail that can be manipulated to allow control over the length (C<sub>16</sub>), a glutamic acid (Glu) linker, a -(CH<sub>2</sub>)<sub>2</sub>- spacer, and a headgroup that contains the bioactive sequence. The tails serve to align the peptide strands and provide a hydrophobic surface for self-association and interaction with other hydrophobic surfaces. The affinity of fractalkine for the synthetic NTFR peptide-amphiphile was investigated with an atomic force microscope (AFM), as this technique is an effective tool in characterizing drug delivery systems.<sup>27</sup> For this, fractalkine was immobilized directly onto the silicon nitride AFM tip and forces were measured between the immobilized fractalkine and bioartificial membranes composed of different concentrations of NTFR peptide-amphiphiles and DPPC. Specificity was established by comparing data to the interaction forces between other adhesion receptors and their ligands. The ultimate goal of this work is to design a drug delivery system that will target only fractalkine and not other adhesion receptors present at the healthy or inflamed endothelium. Therefore, as a first step it is important to show that the NTFR bullet will bind only to the target and not to other receptors expressed on the surface of endothelial cells. Integrins were chosen as a control system as they are adhesion receptors expressed by healthy and inflamed endothelial cells. For this experiment the receptor of choice was the  $\alpha_5\beta_1$  integrin. Bioartificial membranes made out of GRGDSP (the ligand for the  $\alpha_5\beta_1$  integrin) or GRGESP (an inactive peptide) peptide-amphiphiles were used to collect adhesion forces with immobilized  $\alpha_5\beta_1$  receptors. Adhesion measurements studied with experimental tools such as the AFM depend on the loading rate and the number of bonds involved. That is why comparisons between different systems measured with different tips involving different number of bonds and at different loading rates are discouraged. Comparisons should be made across different systems only if the measurements involved correspond to a similar number of bonds (thus it is easier to compare single-molecule bonds) and at the same loading rate. In the present study all measurements, with the fractalkine system and the integrin system, have been performed at the same loading rate and with tips that have similar radii. However, variability from one tip to another is expected as the nominal radius of the tips can vary from 5 to 40 nm according to the manufacturer's specifications. Therefore, qualitative comparisons between different tips remain valid; however, quantitative comparisons should be made only between measurements performed with the same tip. For this reason all measurements were performed with three different tips, which may have different radii, to demonstrate variations from one tip to another.

Force measurements were performed at a constant loading rate of 60 nN/s and the adhesive interactions were studied at the collective level, when each adhesion event corresponds to the rupture of multiple biomolecular bonds. It would be desirable to identify the number of individual bonds involved in each adhesion event. However, this is not trivial. One would need to know the geometry of the system, that is, the

exact radius of the AFM tip, and the percentage of fractalkine surface coverage for every tip. Unfortunately, the exact radius of the AFM tip is not known and there is no easy way to calculate the fractalkine surface coverage for every AFM tip considering its small radius. Thus, a more reliable way to determine the number of individual bonds involved in each adhesion event would be to perform single-molecule force spectroscopy in order to identify the force quantum for a single receptor–ligand pair and from that to deduce the number of bonds involved in each adhesion event. In addition, single-molecule AFM measurements can be carried out in a range of loading ranges to give a measure of the spontaneous dissociation (off rate) reaction rate ( $k_{\text{off}}^{\circ}$ ), as this is a parameter of prime interest for any biological ligand–receptor system. We, for example, have determined the  $k_{\text{off}}^{\circ}$  for the  $\alpha_5\beta_1$ -GRGDSP system, and the results from the AFM study were in agreement with solution off rates reported for the  $\alpha_5\beta_1$  integrins.<sup>28</sup> However, the present paper focuses on collective (multiple) interactions at a fixed loading rate, and in general, an increase in the adhesion force measured here corresponds to an increase in the affinity of the system.

Our results demonstrate that the receptor mimicking peptide-amphiphile (NTFR peptide-amphiphile) can serve as a bullet for fractalkine targeting and can effectively functionalize the exterior of liposomes for targeted drug delivery applications. Current work in our lab focuses on engineering stealth liposomes [liposomes covered with poly(ethylene glycol)] that will utilize the NTFR peptide-amphiphile as a bullet to specifically target fractalkine expressed on the surface of inflamed endothelial cells.

## Materials and Methods

**Preparation and Characterization of Bioartificial Membranes.** DSPE (1,2-distearoyl-*sn*-glycero-3-phosphatidylethanolamine) and DPPC were obtained from Avanti Polar Lipids, Inc. (Alabaster, AL). The peptide headgroup NTFR (Gln-Phe-Pro-Glu-Ser-Val-Thr-Glu-Asn-Phe-Glu-Tyr-Asp-Asp-Leu-Ala-Glu-Ala) corresponds to residues 3–20 of the N-terminus of CX<sub>3</sub>CR1 (SWISS-PROT accession number P49238). The peptide amphiphiles (C<sub>16</sub>)<sub>2</sub>-Glu-C<sub>2</sub>-NTFR, (C<sub>16</sub>)<sub>2</sub>-Glu-C<sub>2</sub>-GRGDSP, and (C<sub>16</sub>)<sub>2</sub>-Glu-C<sub>2</sub>-GRGESP were synthesized according to literature protocols.<sup>29</sup> These peptide-amphiphiles will be referred as NTFR, GRGDSP, and GRGESP, respectively, in the remainder of the text.

Pure peptide-amphiphiles were dissolved at approximately 1 mg/mL in a 99:1 chloroform/methanol solution and stored at 4 °C. The solution was heated to room temperature prior to use. Langmuir–Blodgett (LB) technique was used to create supported bioactive bilayer membranes. LB film depositions were done on a KSV 5000 LB system (KSV Instruments, Helsinki, Finland). All the depositions were done at 41–45 mN/m, which is well below the collapse pressure of 63 mN/m. The pH of the water subphase, when necessary, was adjusted to 10 by adding 30% NH<sub>4</sub>OH. Deposition speed for both the up and down strokes was 1 mm/min. Freshly cleaved mica disks of radius 7.5 mm were used as substrates for the supported bilayer membranes. The DSPE layer was deposited first at the upstroke to make mica

surfaces hydrophobic. The second layer with peptide-amphiphiles was deposited in the down stroke. Transfer ratios for both layers were calculated to be in the range 0.8–1, indicating that monolayers were deposited on mica surfaces with minimal disruption. The resulting supported bilayer membranes were transferred into glass vials under water. Care was taken to avoid exposing the surface to air, as they rearrange to form multilayers.<sup>30</sup>

AFM characterization of the LB films was done with a Digital Instruments Nanoscope III system equipped with a fluid cell for tapping mode (Digital Instruments, Santa Barbara, CA). Images were obtained in tapping mode in DI water, pH 7, by use of standard 100  $\mu\text{m}$  V-shaped silicon nitride AFM cantilevers with pyramidal tips (Digital Instruments) of nominal radius 5–40 nm and nominal spring constant 0.58 N/m. The amplitude set point was kept as high as possible to minimize the influence of sample properties on the topographic contrast.<sup>31</sup>

**Fractalkine Immobilization.** Fractalkine molecules were immobilized on AFM cantilevers by functionalizing the AFM tips with a monoclonal antihistidine antibody that specifically recognized the polyhistidine epitope tag at the end of the mucin domain of fractalkine, thus presenting the chemokine domain of fractalkine at the interface.<sup>32</sup> For this, AFM cantilevers were first washed with ethanol and then placed under a low-wavelength UV light in the presence of water vapor for 30 min. After cleaning, cantilevers were washed with phosphate-buffered saline (PBS) (Life Technologies, Rockville, MD) and incubated overnight with a 10  $\mu\text{g}/\text{mL}$  solution of monoclonal antihistidine antibody (R&D Systems, Minneapolis, MN) in 50 mM Tris-HCl (pH 9.5) at 4 °C. The cantilevers were then washed with PBS and incubated with human fractalkine (1.25  $\mu\text{g}/\text{mL}$  in PBS) with a carboxy tail polyhistidine epitope tag (R&D Systems, Minneapolis, MN) for 2 h at room temperature. The cantilevers were washed with PBS and used immediately.

**$\alpha_5\beta_1$  Integrin Immobilization.** Purified human  $\alpha_5\beta_1$  integrins were purchased from Chemicon International (Temeucula, CA) and immobilized according to the protocol that was described elsewhere.<sup>33</sup>

**Adhesion Force Measurements.** Surface force measurements were performed on a commercial AFM, a Nanoscope III (Digital Instruments, Santa Barbara, CA), in contact mode at a loading rate, defined as the spring constant of the cantilever times the velocity of the piezo, of 60 nN/s, by use of standard 200  $\mu\text{m}$  V-shaped silicon nitride AFM cantilevers with pyramidal tips (Digital Instruments) of nominal radius 5–40 nm and a nominal spring constant of 0.06 N/m. Data were recorded as the two surfaces, the sample surface and the probe tip, were brought into contact and then pulled apart. The adhesion force or the “pull-off” force is defined as the minimum force required to separate two surfaces. All adhesion force measurements were carried out at room temperature and at pH 6.5–7. To minimize the drift effects, AFM was warmed for at least half an hour before an experiment. AFM force data were converted to force–distance curves by the DI-AFM software (Nanoscope III). The hydrodynamic drag force was included on all force measurements.<sup>28</sup>

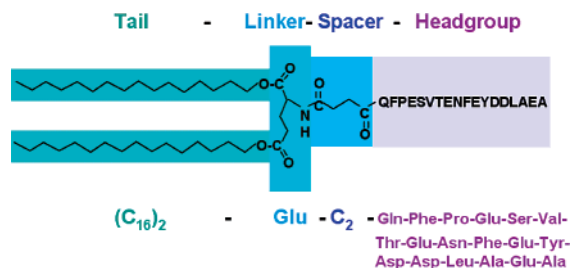


**Figure 2.** Structure of the NTFR peptide-amphiphile.

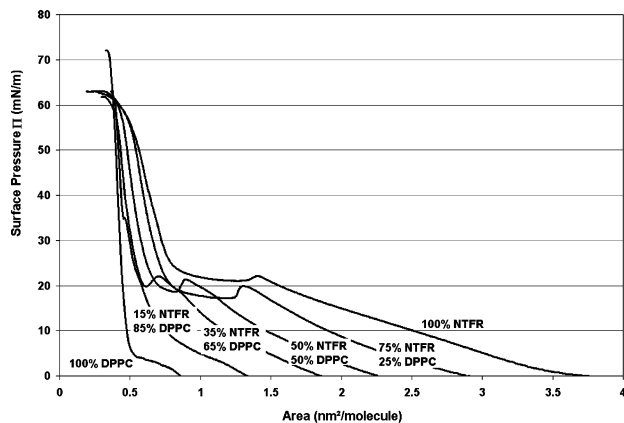


**Figure 3.** Surface pressure–area isotherms of NTFR peptide-amphiphiles and DPPC on a DI water subphase at pH 10 and room temperature.

### Results and Discussion

A schematic diagram of the NTFR peptide-amphiphile is shown in Figure 2. As a first attempt the NTFR peptide was connected to the spacer at its N-terminus. Future designs will connect the NTFR peptide to the spacer at its C-terminus. The NTFR peptide-amphiphiles need to be able to assemble with the DPPC phospholipids in order to be incorporated in the membrane of liposomes with minimal disruption. The assembling properties of the NTFR peptide-amphiphile with different mixtures of DPPC were characterized by measuring pressure–area Langmuir–Blodgett isotherms (Figure 3). A Langmuir isotherm of an amphiphile at the air–water interface can be considered a two-dimensional analogue to pressure–volume isotherms in three-dimensional space. For the pure NTFR isotherm, a large expanded phase was detectable at 3.6 nm<sup>2</sup>/molecule that underwent a noticeable transition at 1.38 nm<sup>2</sup>/molecule and was compressed into a condensed phase at surface pressures larger than 25 mN/m before it collapsed above 60 mN/m. For the NTFR–DPPC mixtures, the surface pressure gradually increased as the NTFR–DPPC monolayers were compressed, and at surface areas of 0.33–0.38 nm<sup>2</sup>/molecule no further compression was possible and the mixed monolayers collapsed at a maximum surface pressure of 62–63 mN/m (72 mN/m for the pure DPPC). The value of 0.33–0.38 nm<sup>2</sup>/molecule is in agreement with that of closely packed tails.<sup>34</sup> Therefore, this number serves as a confirmation that pure amphiphiles are successfully placed on the interface. The high collapse pressures indicate the presence of highly ordered and stable monolayers. These data confirm that NTFR, DPPC, and their mixtures possess high assembly properties.

Figure 3 shows that there is a “hump” on the isotherms of the peptide-amphiphiles that is more pronounced in the

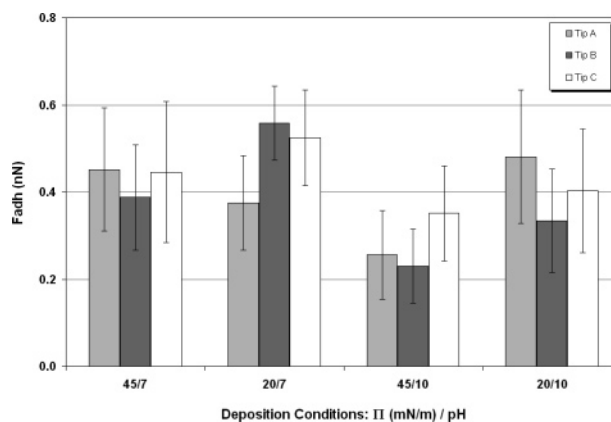


**Figure 4.** Effect of deposition pressure and pH of the water subphase on adhesion between immobilized fractalkine and NTFR amphiphiles measured in DI water at pH 6.5–7. Data correspond to the average value of 75–100 force measurements on each surface. The error bars show standard deviations and reflect the fact that the number of pairs that interact every time the two surfaces are brought into contact can vary from one measurement to another. Deposition conditions do not seem to affect adhesion, within the standard deviation of measurements, with the exception of  $\Pi = 45$  mN/m and pH = 10, where there is a small decrease.

case of NTFR–DPPC mixtures. This hump has also been observed on the isotherms of NTFR peptide-amphiphiles with mixtures of lipidated short poly(ethylene glycol) (PEG120) molecules.<sup>35</sup> Previous studies have shown that peptide-amphiphiles with long headgroups undergo a phase transition as their headgroups change conformations from a globular or folded conformation to an extended one when compressed into monolayers at the air–water interface, which appears as a “hump” on the LB isotherm.<sup>33,36</sup>

The effect of deposition parameters, such as pressure and pH, on the adhesion strength of the NTFR–fractalkine system is shown in Figure 4. For that, pure NTFR membranes were deposited at different combinations of deposition pressure ( $\Pi$ ) and water subphase pH and forces were collected between these surfaces and immobilized fractalkine at pH 6.5–7 (so that all measurements were performed at physiological range). Two different pressures and pHs were used. The deposition pressure of 45 mN/m corresponds to the condensed phase and the deposition pressure of 20 mN/m to the expanded phase. Two different pH values of 7 and 10 were used for the water subphase. With the exception of surfaces that were prepared at a deposition pressure of 45 mN/m and pH 10, which showed a small decrease in adhesion, all other surfaces gave comparable adhesion strength within the standard deviations of the measurements. Therefore a preparation method was followed where the pH of the water subphase was kept at 7 and the deposition pressure was at 45 mN/m that corresponds to a solidlike well-ordered monolayer.

The affinity of fractalkine for the synthetic NTFR peptide-amphiphile was investigated by measuring their adhesion force. Retraction AFM force–distance curves, after the fractalkine–100% NTFR surfaces were in contact, are shown in Figure 5. Figure 5A shows two kinds of force profiles. Curve 1 shows a single peak: therefore in this case all bonds involved in this adhesion event break simultaneously. Curves 2 and 3 in Figure 5A show a stepwise profile. In

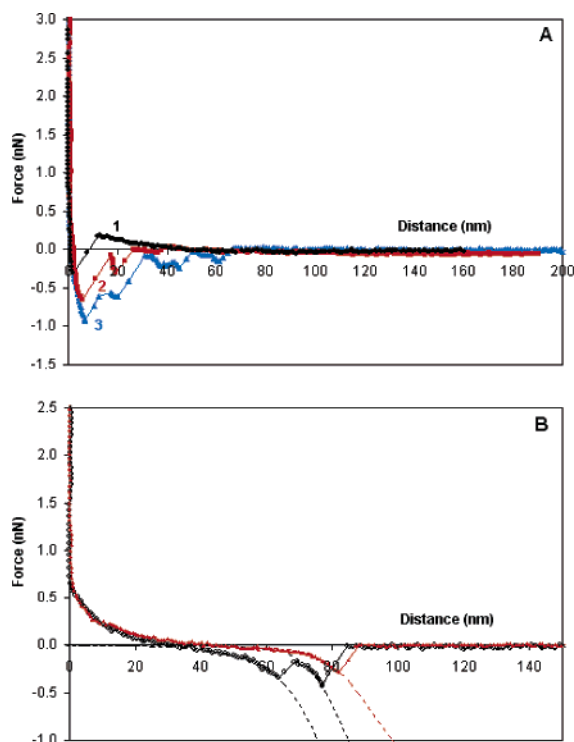


**Figure 5.** (A) Retraction force–distance curves between immobilized fractalkine molecules on the AFM tip and NTFR peptide-amphiphile bilayer membranes measured in DI water at pH 6.5–7 and at a loading rate of 60 nN/s. Curves 1 and 2 have been measured with the same tip and surface. (B) Force extension curves for the fractalkine–NTFR complex. These two curves were collected with the same tip and surface in DI water at pH 6.5–7 and at a loading rate of 60 nN/s. The dotted lines are the modified WLC fits to the experimental data.

this case the ligand–receptor pairs do not break at once but in multiple steps, thus producing a stepwise return to zero force. These separation profiles are independent of the tip used. For example, curves 1 and 2 were collected with the same tip and surface. Thus, the same tip can give rise to a single peak or multiple peaks, indicating that every time the tip and surface are in contact a different number of pairs can interact that may or may not break simultaneously. The fact that at every adhesion event the number of bonds involved is not constant gives rise to the standard deviations in the adhesion forces reported in this study. A small percentage of force measurements (about 4%) showed stretching of the fractalkine–NTFR complex. Two force profiles that demonstrate stretching are shown in Figure 5B. Four different models of polymer elasticity were used to fit the data: the wormlike chain (WLC),<sup>37</sup> the freely joined chain (FJC),<sup>38</sup> the modified WLC,<sup>39</sup> and the modified FJC model.<sup>40</sup> The best fit to the data was given by the modified WLC model (dotted lines in Figure 5B):

$$x(F) = L_c \left[ 1 - \frac{1}{2} \left( \frac{k_B T}{Fl} \right)^{1/2} + \frac{F}{S} \right] \quad (1)$$

where  $x$  is the extension,  $F$  is the external force,  $L_c$  is the contour length, which is equal to  $nl$ ,  $n$  is the total number of statistical segments,  $l$  is the persistence length (the length of the statistical segment),  $k_B$  is the Boltzmann constant,  $T$  is the temperature, and  $S$  is the elastic stretch modulus, which

is equal to  $k_s L_c$ , where  $k_s$  is the elasticity of the system. A value of 0.37 nm was used for  $l$ , which is the contour length of a peptide residue.<sup>41</sup> If the persistence length was also allowed to vary in the fitting, then  $l = 0.37 \pm 0.02$  nm. Four different peaks were measured and the fits to the data gave the following values:  $L_{c1} = 28.8 \pm 5.3$  nm,  $k_{s1} = 51.7 \pm 6.2$  pN/nm;  $L_{c2} = 57.4 \pm 4.4$  nm,  $k_{s2} = 49.7 \pm 18.1$  pN/nm;  $L_{c3} = 72.6 \pm 1.7$  nm,  $k_{s3} = 63.6 \pm 26$  pN/nm; and  $L_{c4} = 83.4 \pm 2.9$  nm,  $k_{s4} = 95.7 \pm 38.9$  pN/nm. In a force extension curve the first fit represents the length of the molecule before any unfolding occurs.<sup>42</sup> The first fit to our data gave a contour length of  $L_{c1} = 28.8 \pm 5.3$  nm, which corresponds to the length of the folded fractalkine–NTFR complex. The length of fractalkine is 29 nm<sup>12</sup> and the length of the NTFR peptide is approximately 6.6 nm (18 amino acids  $\times$  0.37 nm/amino acid). The fit to the second peak gave a contour length of  $L_{c2} = 57.4 \pm 4.4$  nm, which corresponds to an increment of approximately 28.6 nm from the first peak and is due to the unfolding of a protein domain. The length of 28.6 nm corresponds to the stretching of  $n = 77$  amino acids and we speculate that this may be due to the unfolding of fractalkine’s N-terminal chemokine module that has 76 amino acids.<sup>5</sup> The third peak gave an increment of approximately 15.2 nm from the second peak and corresponds to the unfolding of 41 amino acids of the stalk region, and the fourth peak added 10.8 nm to the length of the complex, which corresponds to an additional stretch of 29 amino acids. Thus, the last two peaks showed stretching of a total of 70 amino acids from the mucin domain, which is less than the total number of 241 amino acids in the stalk region.<sup>5</sup> The elasticity of the folded fractalkine–NTFR complex was found to be  $k_{s1} = 51.7 \pm 6.2$  pN/nm. The elasticity of the system is a measure of its extensibility and can be thought as the spring constant of the system. A direct correlation between the elasticity of the system and the molecular spring constant of a single receptor–ligand pair is difficult to obtain since the number of bonds involved is unknown.

AFM adhesion forces between fractalkine molecules immobilized on the AFM tip and membranes of NTFR peptide-amphiphiles mixed with DPPC demonstrated strong adhesion for the synthetic NTFR molecule, but the fractalkine–DPPC adhesion was minimal (Figure 6). The adhesion was increased for surfaces that had both NTFR and DPPC phospholipids, especially for the concentration of 75% NTFR–25% DPPC, compared to 100% NTFR. Since the DPPC alone did not show any adhesion with the fractalkine, we speculate that the increased adhesion in the case of the 75% NTFR–25% DPPC surfaces is due to the shorter DPPC providing more space for the NTFR headgroup to bend and expose the full sequence at the interface versus the 100% NTFR interfaces, which were more compact. This result is in agreement with previous work that showed that the presence of a shorter molecule at the interface can provide more space for the peptide-amphiphile headgroup to bend and expose the binding sequence, thus increasing the adhesion.<sup>33</sup> However, as the DPPC concentration increased to 50%, the adhesion was still higher compared to the 100% NTFR surface but smaller compared to the 75% NTFR–

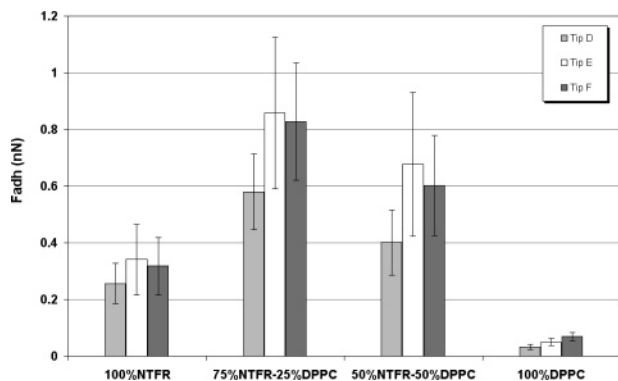


**Figure 6.** Adhesion measurements between immobilized fractalkine and different surfaces measured in DI water at pH 6.5–7. Each column is the average of 30–50 measurements on each surface. The error bars show standard deviations and reflect the fact that the number of pairs that interact may vary from one measurement to another. Fractalkine does not bind to the DPPC surfaces. Mixtures of 75% NTFR–25% DPPC give an increase in adhesion compared to pure NTFR.

25% DPPC. The observed decrease in adhesion from 75% NTFR–25% DPPC to 50% NTFR–50% DPPC could be due to the possibility that the higher concentration of DPPC at the interface increased the chances for fractalkine to interact with the DPPC and thus for the overall adhesion to decrease since the DPPC molecules did not show any affinity for fractalkine.

AFM was used to characterize surface topography of the supported bioartificial membranes constructed from NTFR–DPPC mixtures and verify miscibility of these amphiphilic molecules. Figure 7 presents topography and phase AFM images of pure NTFR surfaces and NTFR–DPPC mixtures that were deposited at pH 7 and 10. All images were taken at room temperature in tapping mode in DI water at pH 7. Phase imaging provides clearer observation of fine features often not revealed by topography and can also act as a real-time contrast enhancement technique. Additionally, phase imaging can detect variations in composition, friction, viscoelasticity, and other properties within the sample, but it cannot provide accurate information about the height of the objects. AFM images of the 100% NTFR (Figure 7A), 75% NTFR–25% DPPC (Figure 7B), and 50% NTFR–50% DPPC (Figure 7C) surfaces deposited at pH 7 showed that the surfaces are smooth and in addition the absence of any features on the phase images of the mixed NTFR–DPPC monolayers demonstrated that the NTFR and DPPC formed well-mixed interfaces at these concentrations. For comparison, AFM images of the 100% NTFR, 75% NTFR–25% DPPC, and 50% NTFR–50% DPPC surfaces deposited at pH 10 are shown in Figure 7D–F, respectively. Cross-sectional analysis of the height images for 75% NTFR–25% DPPC (Figure 7E) and 50% NTFR–50% DPPC (Figure 7C) indicated that the height differences between the shorter (DPPC) domains, shown with a dark color, and the taller (NTFR) domains, shown with a light color, are  $3.06 \pm 0.50$  nm, which is within the upper limit of the 6.2 nm height difference between the NTFR and DPPC for fully extended headgroups. The NTFR headgroup was calculated to be approximately 7.36 nm [18 amino acids  $\times$  0.37 nm/amino acid,<sup>41</sup> plus 0.7 nm for the length of the (Glu) linker and

(CH<sub>2</sub>)<sub>2</sub> spacer<sup>43</sup>] and the DPPC headgroup was found to be  $1.15 \pm 0.15$  nm for solid-phase monolayers.<sup>44</sup> Small dark areas of an average depth of  $8.75 \pm 0.92$  nm were observed on the 100% NTFR monolayer that was deposited at pH 10 (Figure 7D). We speculate that these areas correspond to missing peptide-amphiphile molecules within the monolayer since the total theoretical length of the fully extended NTFR peptide-amphiphile was calculated to be 8.88 nm (7.36 nm for NTFR headgroup plus  $1.52 \pm 0.1$  nm for a C-16 chain thickness in a solid-phase monolayer<sup>44</sup>).

To test the specificity of the NTFR peptide-amphiphile for fractalkine, adhesion forces were collected between fractalkine and an adhesion receptor that is also expressed on the surface of endothelial cells ( $\alpha_5\beta_1$  integrins) and membranes composed of 75% NTFR and 25% DPPC (the surface composition that demonstrated the highest adhesion in Figure 6). Figure 8 shows that the mean adhesion force of NTFR for fractalkine is about 3–4-fold stronger compared to the mean force measured for the  $\alpha_5\beta_1$  integrin. In addition, fractalkine does not bind to surfaces that have only DPPC phospholipids, as shown in Figure 6.

To confirm that the strength of adhesion measured between NTFR and the integrin is not comparable to the specific interaction between the  $\alpha_5\beta_1$  receptor and its ligand (GRGDSP), forces were collected between  $\alpha_5\beta_1$  integrins and the following surfaces: GRGDSP, GRGESP (an inactive peptide, used as a negative control to demonstrate lack of specificity for the integrins), NTFR, and 75% NTFR–25% DPPC. Figure 9 demonstrates that the NTFR– $\alpha_5\beta_1$  interaction is much smaller than the specific GRGDSP– $\alpha_5\beta_1$  interaction and is of the same value or smaller than the nonspecific interaction measured between the inactive GRGESP and  $\alpha_5\beta_1$ . In addition, Figures 8 and 9 show that the NTFR–fractalkine adhesion is comparable to the interaction of the adhesion receptor  $\alpha_5\beta_1$  with its ligand GRGDSP.

## Conclusions

In this study we have designed and engineered a peptide-amphiphile that specifically targets fractalkine, an adhesion molecule expressed on the surface of inflamed endothelial cells. For the development of a fractalkine-targeting peptide-amphiphile we focused on the N-terminus of CX<sub>3</sub>CR1, the fractalkine receptor. The design was based on the hypothesis that a peptide-amphiphile that mimics a fragment of the N-terminus of the fractalkine receptor (NTFR peptide-amphiphile) will recognize and specifically bind to fractalkine.

Bioartificial membranes were constructed from mixtures of NTFR peptide-amphiphiles and DPPC phospholipids, and the affinity and specificity of fractalkine for the synthetic NTFR peptide-amphiphile were investigated with an AFM. Fractalkine was immobilized directly onto the silicon nitride AFM tip, and forces were collected between the immobilized fractalkine and bioartificial membranes composed of different concentrations of NTFR peptide-amphiphiles and DPPC.

Results demonstrated that the adhesion measured was independent of the deposition conditions used to prepare the bioartificial membranes for the range of conditions that was

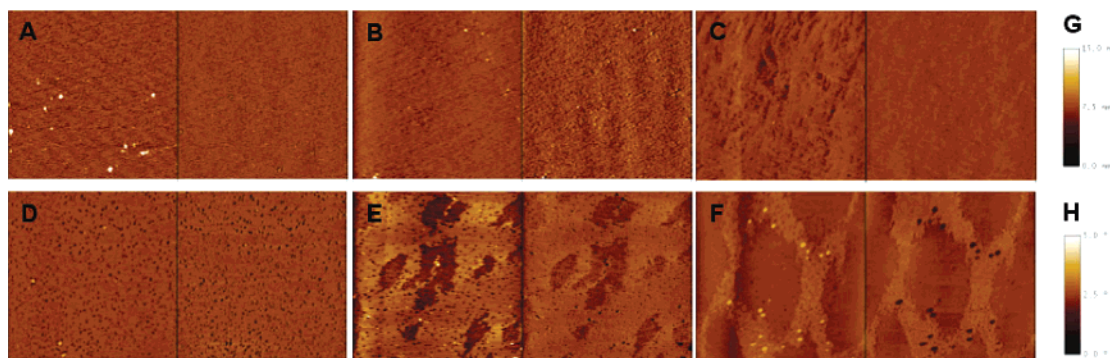


**Figure 7.** Height (left) and phase (right) images (tapping-mode AFM in DI water at pH 6.5–7) of NTFR–DPPC mixtures, deposited at room temperature. All images are  $10 \times 10 \mu\text{m}$  with the exception of image F, which is  $15 \times 15 \mu\text{m}$ . Third-order flattening was applied to all the images. (A) 100% NTFR deposited at pH 7. (B) 75 mol % NTFR and 25 mol % DPPC deposited at pH 7. (C) 50 mol % NTFR and 50 mol % DPPC deposited at pH 7. (D) 100% NTFR deposited at pH 10. (E) 75 mol % NTFR and 25 mol % DPPC deposited at pH 10. (F) 50 mol % NTFR and 50 mol % DPPC deposited at pH 10. (G) 15 nm scale bar for all height images. (H) 5° scale bar for all phase images.

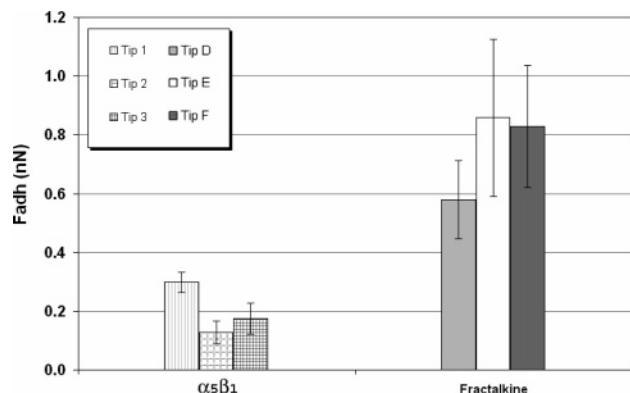


**Figure 8.** Adhesion measurements between surfaces with 75% NTFR–25% DPPC and AFM tips functionalized with  $\alpha_5\beta_1$  integrins or fractalkine. The measurements with the integrins were performed in 1 mM  $\text{MnCl}_2$  solution at pH 6.5–7, as  $\text{Mn}^{2+}$  ions have been shown to activate isolated  $\alpha_5\beta_1$  integrins.<sup>45</sup> Measurements with fractalkine tips were collected in DI water at pH 6.5–7. Each column is the average of 30–50 measurements on each surface. The error bars show standard deviations and reflect the fact that the number of pairs that interact may vary from one measurement to another. The NTFR binds preferentially to fractalkine.

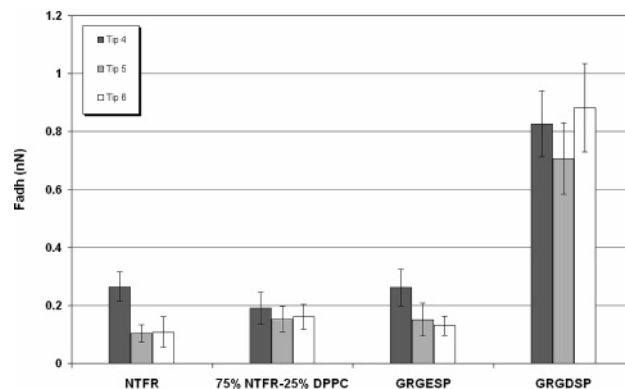


**Figure 9.** Adhesion measurements between immobilized  $\alpha_5\beta_1$  integrins and different surfaces in 1 mM  $\text{MnCl}_2$  solution at pH 6.5–7. Data correspond to the average value of 30–40 force measurements on each surface. The error bars show standard deviations and reflect the fact that the number of pairs that interact every time the two surfaces are brought into contact can vary from one measurement to another.  $\alpha_5\beta_1$  integrins bind strongly to their specific ligand, GRGDSP. The integrins do not bind to the inactive GRGESP surface, NTFR, or 75% NTFR–25% DPPC surfaces.

examined. Therefore, a protocol was followed that allowed the preparation of membranes at a physiological pH and a high enough pressure that gave rise to solidlike well-ordered interfaces.

The NTFR–fractalkine force profiles gave rise to a single or multiple peaks that were independent of the tip used and demonstrated that the number of bonds involved in every adhesion event can vary and that multiple bonds may break simultaneously or in multiple steps. A small percentage of force profiles (about 4%) demonstrated stretching of the NTFR–fractalkine complex. A total of four different peaks were measured, and fits to the modified WLC model showed that the first peak corresponded to the length of the NTFR–fractalkine complex, the second peak to the unfolding of fractalkine’s chemokine domain, and the third and fourth peaks to the unfolding of portions of the mucin stalk.

A ratio of 3:1 NTFR:DPPC phospholipid gave the highest fractalkine adhesion, even better than 100% NTFR (a detailed analysis on the effect of the DPPC concentration on the NTFR–fractalkine adhesion was beyond the scope of this study). Since the DPPC molecules did not show any adhesion with fractalkine, we propose that the increased adhesion for

the NTFR–DPPC surfaces is due to the shorter DPPC molecules giving the NTFR headgroup space to bend and expose the full bioactive sequence at the interface, which allows increased adhesion to fractalkine.

The specificity of the NTFR for fractalkine was examined by comparing the NTFR–fractalkine interaction to that of another adhesion receptor expressed on the surface of endothelial cells, the  $\alpha_5\beta_1$  integrin. Adhesion measurements were collected between the integrin and the following surfaces: GRGDSP (the specific ligand for  $\alpha_5\beta_1$ ), GRGESP (an inactive peptide that served as a negative control), NTFR, and 75% NTFR–25% DPPC. A comparison of these measurements to the interaction of fractalkine with 75% NTFR–25% DPPC surfaces demonstrated that the NTFR peptide-amphiphile binds preferentially to fractalkine with an affinity that is comparable to the  $\alpha_5\beta_1$ –GRGDSP specific interaction.

Our results demonstrate that the receptor-mimicking NTFR peptide-amphiphile self-assembles with phospholipids and gives a strong interaction with fractalkine. Upon further testing, the NTFR could be used as a magic bullet for selective drug delivery to fractalkine.

**Acknowledgment.** Partial financial support by National Research Service Award T32 GM08515 from the NIH and from MRSEC under NSF DMR 021 3695 is gratefully acknowledged. Acknowledgment is also made to the donors of the Petroleum Research Fund, administered by the American Chemical Society, for partial support of this research under 39120-G4.

## References and Notes

- (1) Torchilin, V. P. *Eur. J. Pharm. Sci.* **2000**, *11*, S81–S91.
- (2) Gregoriades, G.; Neerunjun, D. E. *Biochem. Biophys. Res. Commun.* **1975**, *65*, 537–544.
- (3) Lasic, D. D. *Liposomes: from physics to applications*; Elsevier: Amsterdam, 1993.
- (4) Woodle, M. C.; Storm, G. *Long circulating liposomes: old drugs, new therapeutics*; Springer-Verlag: Berlin, 1998.
- (5) Bazan, J. F.; Bacon, K. B.; Hardiman, G.; Wang, W.; Soo, K.; Rossi, D.; Greaves, D. R.; Zlotnik, A.; Schall, T. J. *Nature* **1997**, *385*, 640–644.
- (6) Pan, Y.; Lloyd, C.; Zhou, H.; Dolich, S.; Deeds, J.; Gonzalo, J.-A.; Vath, J.; Gosselin, M.; Ma, J.; Dussault, B.; Woolf, E.; Alperin, G.; Culpepper, J.; Gutierrez-Ramos, J. C.; Gearing, D. *Nature* **1997**, *387*, 611–617.
- (7) Harrison, J. K.; Jiang, Y.; Chen, S.; Xia, Y.; Maciejewski, D.; Mcnamara, R. K.; Streiti, W. J.; Salafra, M. N.; Adhikari, S.; Thompson, D. A.; Botti, P.; Bacon, K. B.; Feng, L. *Proc. Natl. Acad. Sci. U.S.A.* **1998**, *95*, 10896–10901.
- (8) Muehlhoefer, A.; Saubermann, L. J.; Gu, X.; Luedtke-Heckenkamp, K.; Xavier, R.; Blumberg, R. S.; Podolsky, D. K.; MacDermott, R. P.; Reinecker, H.-C. *J. Immunol.* **2000**, *164*, 3368–3376.
- (9) Kanazawa, N.; Nakamura, T.; Tashiro, K.; Muramatsu, M.; Morita, K.; Yoneda, K.; Inaba, K.; Imamura, S.; Honjo, T. *Eur. J. Immunol.* **1999**, *29*, 1925–1932.
- (10) Imai, T.; Hieshima, K.; Haskell, C.; Baba, M.; Nagira, M.; Nishimura, M.; Kakizaki, M.; Takagi, S.; Nomiyama, H.; Schall, T. J.; Yoshie, O. *Cell* **1997**, *91*, 521–530.
- (11) Combadiere, C.; Salzwedel, K.; Smith, E. D.; Tiffany, H. L.; Berger, E. A.; Murphy, P. M. *J. Biol. Chem.* **1998**, *273*, 23799–23804.
- (12) Fong, A. M.; Erickson, H. P.; Zachariah, J. P.; Poon, S.; Schamberg, N. J.; Imai, T.; Patel, D. D. *J. Biol. Chem.* **2000**, *275*, 3781–3786.
- (13) Haskel, C. A.; Cleary, M. D.; Charo, I. F. *J. Biol. Chem.* **2000**, *275*, 34183–34189.
- (14) Fong, A. M.; Alam, S. M.; Imai, T.; Haribabu, B.; Patel, D. D. *J. Biol. Chem.* **2002**, *277*, 19418–19423.
- (15) Gayle, R. B.; Sleath, P. R.; Srinivason, S.; Birks, C. W.; Weerawarna, K. S.; Cerretti, D. P.; Kozlosky, C. J.; Nelson, N.; Vandebos, T.; Beckmann, M. P. *J. Biol. Chem.* **1993**, *268*, 7283–7289.
- (16) Monteclaro, F. S.; Charo, I. F. *J. Biol. Chem.* **1996**, *271*, 19084–19092.
- (17) Monteclaro, F. S.; Charo, I. F. *J. Biol. Chem.* **1997**, *272*, 23186–23190.
- (18) Wu, L. J.; Ruffing, N.; Shi, X. J.; Newman, W.; Soler, D.; Mackay, C. R.; Qin, S. X. *J. Biol. Chem.* **1996**, *271*, 31202–31209.
- (19) Pease, J. E.; Wang, J.; Ponath, P. D.; Murphy, P. M. *J. Biol. Chem.* **1998**, *273*, 19972–19976.
- (20) Blanpain, C.; Doranz, B. J.; Vakili, J.; Rucker, J.; Govaerts, C.; Baik, S. S. W.; Lorthioir, O.; Migeotte, I.; Libert, F.; Baleux, F.; Vassart, G.; Doms, R. W.; Parmentier, M. *J. Biol. Chem.* **1999**, *274*, 34719–34727.
- (21) Hemmerich, S.; Paavola, C.; Bloom, A.; Bhakta, S.; Freedman, R.; Grunberger, D.; Krstenansky, J.; Lee, S.; McCarley, D.; Mulkins, M.; Wong, B.; Pease, J.; Mizoue, L.; Mirzadegan, T.; Polsky, I.; Thompson, K.; Handel, T. M.; Jarnagin, K. *Biochemistry* **1999**, *38*, 13013–13025.
- (22) Clubb, R. T.; Omichinski, J. G.; Clore, G. M.; Gronenborn, A. M. *FEBS Lett.* **1994**, *338*, 93–97.
- (23) Skelton, N. J.; Quan, C.; Reilly, D.; Lowman, H. *Struct. Folding Des.* **1999**, *7*, 157–168.
- (24) Mizoue, L. S.; Bazan, J. F.; Johnson, E. C.; Handel, T. M. *Biochemistry* **1999**, *38*, 1402–1414.
- (25) Mayer, K. L.; Stone, M. J. *Biochemistry* **2000**, *39*, 8382–8395.
- (26) Ye, J.; Kohli, L. L.; Stone, M. J. *J. Biol. Chem.* **2000**, *275*, 27250–27257.
- (27) Garg, A.; Kokkoli, E. *IEEE Eng. Med. Biol. Mag.* **2005**, *24*, 87–95.
- (28) Kokkoli, E.; Ochsenhirt, S. E.; Tirrell, M. *Langmuir* **2004**, *20*, 2397–2404.
- (29) Berndt, P.; Fields, G. B.; Tirrell, M. *J. Am. Chem. Soc.* **1995**, *117*, 9515–9522.
- (30) Hansma, H. G.; Clegg, D. O.; Kokkoli, E.; Oroudjev, E.; Tirrell, M. *Methods Cell Biol.* **2002**, *69*, 163–193.
- (31) Burnham, N. A.; Behrend, O. P.; Oulevey, F.; Gremaud, G.; Gallo, P.-J.; Gourdon, D.; Dupas, E.; Kulik, A. J.; Pollock, H. M.; Briggs, G. A. D. *Nanotechnology* **1997**, *8*, 67–75.
- (32) Haskell, C. A.; Cleary, M. D.; Charo, I. F. *J. Biol. Chem.* **1999**, *274*, 10053–10058.
- (33) Mardilovich, A.; Kokkoli, E. *Biomacromolecules* **2004**, *5*, 950–957.
- (34) Tanford, C. *The hydrophobic effect: formation of micelles and biological membranes*; John Wiley and Sons: New York, 1980.
- (35) Mardilovich, A.; Kokkoli, E. *Langmuir* **2004**, submitted for publication.
- (36) Dillow, A. K.; Ochsenhirt, S. E.; McCarthy, J. B.; Fields, G. B.; Tirrell, M. *Biomaterials* **2001**, *22*, 1493–1505.
- (37) Bustamante, C.; Marko, J. F.; Siggia, E. D.; Smith, S. *Science* **1994**, *265*, 1599–1600.
- (38) Butt, H.-J.; Kappl, M.; Mueller, H.; Raiteri, R. *Langmuir* **1999**, *15*, 2559–2565.
- (39) Odijk, T. *Macromolecules* **1995**, *28*, 7016–7018.
- (40) Smith, S. B.; Finzi, L.; Bustamante, C. *Science* **1992**, *258*, 1122–1126.
- (41) Idiris, A.; Alam, M. T.; Ikai, A. *Protein Eng.* **2000**, *13*, 763–770.
- (42) Fisher, T. E.; Marszalek, P. E.; Fernandez, J. M. *Nat. Struct. Biol.* **2000**, *7*, 719–724.
- (43) Dori, Y.; Bianco-Peled, H.; Satija, S. K.; Fields, G. B.; McCarthy, J. B.; Tirrell, M. *J. Biomed. Mater. Res.* **2000**, *50*, 75–81.
- (44) Brumm, T.; Naumann, C.; Sackmann, E.; Rennie, Ar.; Thomas, R. K.; Kanellas, D.; Penfold, J.; Bayerl, T. M. *Eur. Biophys. J.* **1994**, *23*, 289–295.
- (45) Fernandez, C.; Clark, K.; Burrows, L.; Shofield, N. R.; Humphries, M. J. *Front. Biosci.* **1998**, *3*, d684–d700.

BM0493537